

Two-dimensional Nb₂O₅ holey nanosheets prepared by a graphene sacrificial template method for high performance Mg²⁺/Li⁺ hybrid ion batteries

Huihuang Huang,^a Guangyu Zhao,^{*b} Naiqing Zhang,^{*b} and Kening Sun^b

- a. School of Chemistry and Chemical Engineering, Harbin Institute of Technology, Harbin, 150001, China.
- b. Academy of Fundamental and Interdisciplinary Sciences, Harbin Institute of Technology, Harbin, 150001, China. E-mail: zhaogy810525@gmail.com; znqmww@163.com.

Experimental Section

Materials: Niobium(V) oxalate hydrate (Alfa Aesar); Phenyl magnesium chloride (PhMgCl, 2M solution in THF, Aladdin); anhydrous aluminum chloride (AlCl₃, Aladdin); anhydrous lithium chloride (LiCl, Aladdin); tetrahydrofuran (THF, Aladdin); poly-vinylidene fluoride (PVDF, Macklin); acetylene black (Shanxi Lizhiyuan Battery Material Co., Ltd); N-methyl-2-pyrrolidone (NMP, Aladdin), magnesium metal foil (Mg, Macklin).

Material synthesis: Graphene oxide (GO) aqueous solution was synthesized according to a modified Hummers method.¹ To obtain two-dimensional Nb₂O₅ holey nanosheets (NO-HNS), 2 mL GO solution (5 mg mL⁻¹) and 45 mL distilled water were mixed through ultrasonic treatment for 1 h. After that, 90 mg Niobium(V) oxalate was dissolved in another 13 mL deionized water and then mixed with GO suspension. Afterwards, the mixture was stirred for another 2 h and transferred to 80 mL Teflon-lined autoclave. Subsequently, the autoclave was sealed and hydrothermally treated at 180 °C for 14 h. The obtained black product was washed with water and ethanol several times, then freeze-dried. Finally, the dried product was heat treated at 750 °C for 2 h under air atmosphere to obtain NO-HNS. For comparison, pristine Nb₂O₅ nanoparticles were also synthesized through the same proceeding without the addition of GO aqueous solution.

Material characterization: The XRD patterns of products were characterized by PANalytical X'Pert PRO with Cu Kα radiation. The morphology and microstructure of products were conducted by Field emission SEM (Hitachi, SU8010) and high resolution TEM (JEM-2100 with an accelerating voltage of 200 kV). The surface area of products was measured by the Brunauer-Emmett-Teller method using ASAP2020. XPS was obtained by Thermo Fisher Scientific K-Alpha (Fisher Scientific Ltd, Nepean, ON).

Preparation of electrolyte: The APC electrolyte for MRBs was prepared according to Oren Mizrahi et al in an argon-filled glove box (< 0.1 ppm of water and oxygen) at room temperature.² Firstly, 1.067 g aluminum chloride slowly dissolved in 12 mL THF (dried by activated 4 Å molecular sieves) under vigorous stirring and kept for 12 h. Subsequently, the transparent solution was added to 8 mL phenyl magnesium chloride (2 M in THF) dropwise under vigorous stirring and kept for another 12 h to obtain the 0.4 M APC electrolyte. Finally, 0.848 g anhydrous LiCl

was dissolved in APC electrolyte to obtain 0.4 M APC–1.0 M LiCl electrolyte for MLIBs.

Electrochemical measurements: Electrochemical performances of NO–HNS and pristine T–Nb₂O₅ were evaluated with 2025–type coin cell which were assembled in an argon–filled glove box, using Mg foil as the reference and counter electrodes. The working electrode slurry was prepared by mixing active materials, acetylene black and poly–vinylidene fluoride (PVDF) binder in a weight ratio of 8:1:1 and N–methyl–2–pyrrolidone (NMP) as solvent. The slurry was coated on copper foil through doctor–balding method and dried at 80 °C in a vacuum oven overnight. The mass loading density of active materials in electrode is 0.7~1.0 mg cm⁻². Microporous membrane (Celgard 2400) was employed as the separator. 0.4 M APC/THF, 0.4 M APC–1.0 M LiCl/THF and 1 M LiPF₆ dissolved in a mixture of ethylene carbonate (EC) and dimethyl carbonate (DMC) (1:1, v/v) were employed as the electrolyte of MRBs, MLIBs and LIBs, respectively. Galvanostatic charge/discharge measurements were performed at ambient temperature by a battery test system (Shenzhen Neware Electronic Co., China) from 0.2–1.8 V vs Mg²⁺/Mg. Cyclic voltammetry (CV) measurements were investigated by CHI 660D electrochemical workstation. The linear sweep voltammetry (LSV) measurement was conducted by the same electrochemical workstation from open circuit potential to 2.2 V. Electrochemical impedance spectroscopy (EIS) measurements were conducted with Princeton Applied Research PARSTAT 2273 advanced electrochemical system with 5 mV amplitude, and the frequency range between 100 kHz and 0.1 Hz at open circuit potential (1.5 V).

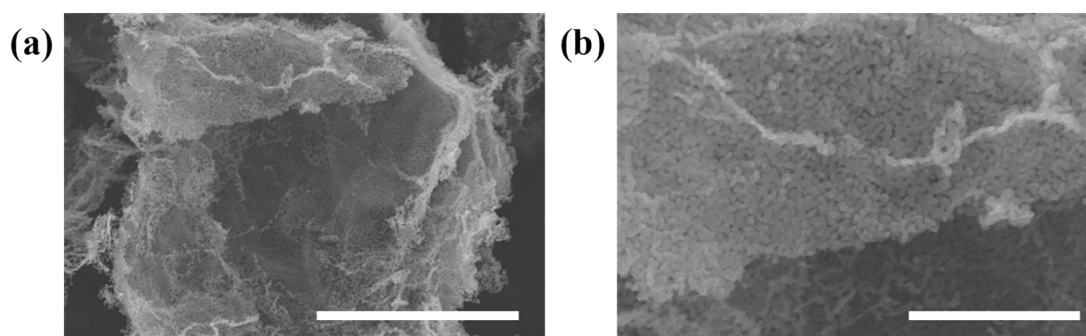


Fig. S1 SEM images of NO–HNS. Scale bars in (a) and (b) are 3 μm and 1 μm, respectively.

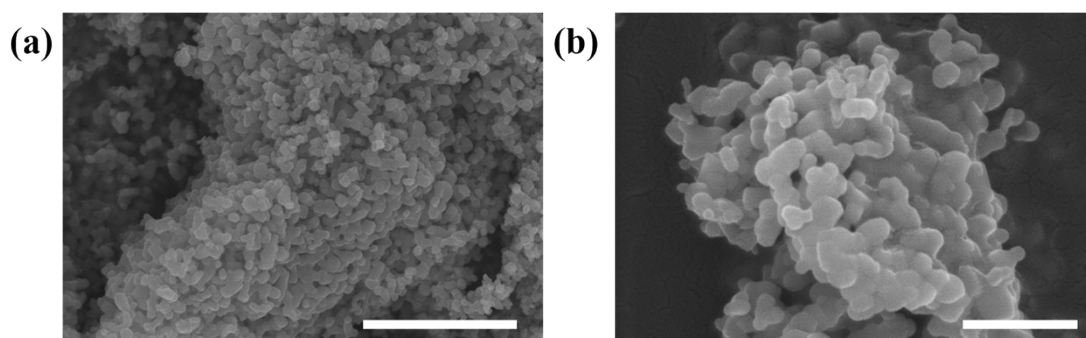


Fig. S2 SEM images of TNO. Scale bars in (a) and (b) are 2 μm and 500 nm, respectively.

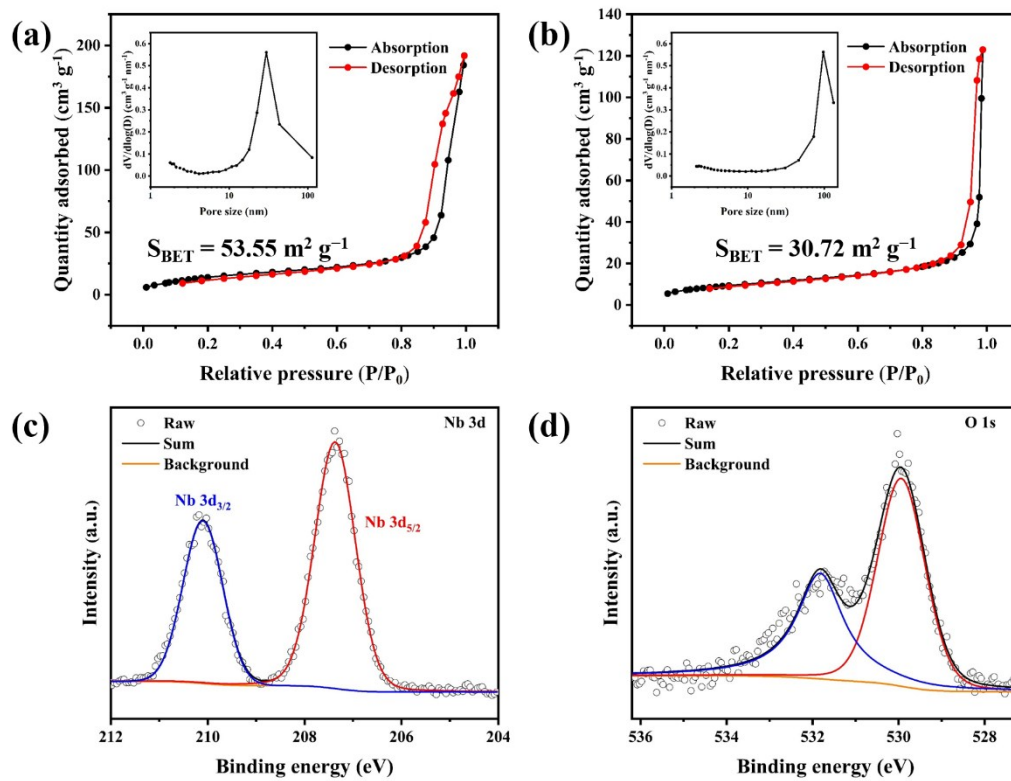


Fig. S3 N₂ adsorption-desorption isotherms of (a) NO-HNS and (b) TNO. The insets in (a) and (b) is pore distribution curves. High resolution XPS with peak fitting of (c) Nb 3d and (d) O 1s for NO-HNS.

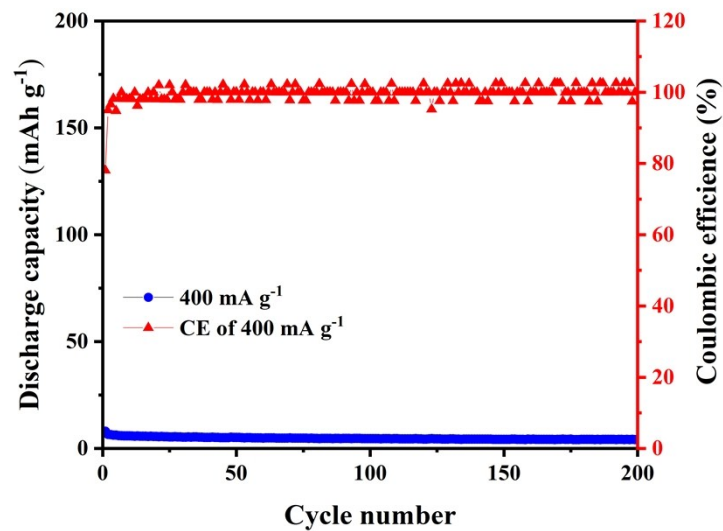


Fig. S4 Cycling performance of NO-HNS in MRB at a current density of 400 mA g⁻¹.

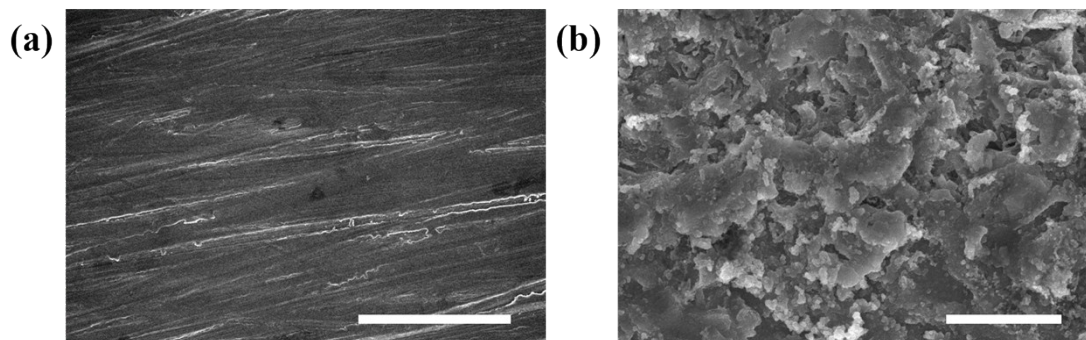


Fig. S5 SEM images of Mg anode obtained from MLIBs. (a) before cycling. (b) after 200 cycles at 400 mA g^{-1} . Scale bars in (a) and (b) are $200 \mu\text{m}$ and $10 \mu\text{m}$, respectively.

Table S1 Comparison of the rate performance of previous cathode materials and this work

Sample	Cut-off voltage (V)	Rate performance Capacity/Current ($\text{mAh g}^{-1}/\text{mA g}^{-1}$)	References
NO-HNS	0.2–1.8	99/1000 72/2000	This work
LiCrTiO_4	0.01–1.8	50/500	S3
V_2MoO_8	0.5–2.4	90/500	S4
$\text{Ti}_3\text{C}_2\text{T}_x$	0.2–2.0	40/1000	S5
$\text{Li}_4\text{Ti}_5\text{O}_{12}$	0.3–1.5	56/350	S6
$\text{TiO}_2(\text{B})$	0.5–1.7	50/1675	S7
TiO_2	0.5–1.7	85/336	S8
MoO_2	0.5–2.0	150/100	S9
$\text{Li}_4\text{Ti}_5\text{O}_{12}$	0.01–1.9	120/300	S10

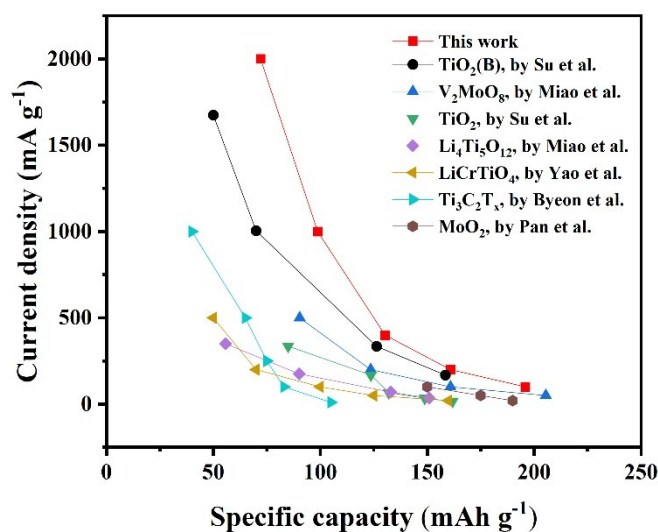


Fig. S6 Comparison of the rate performance of previous cathode materials and this work.

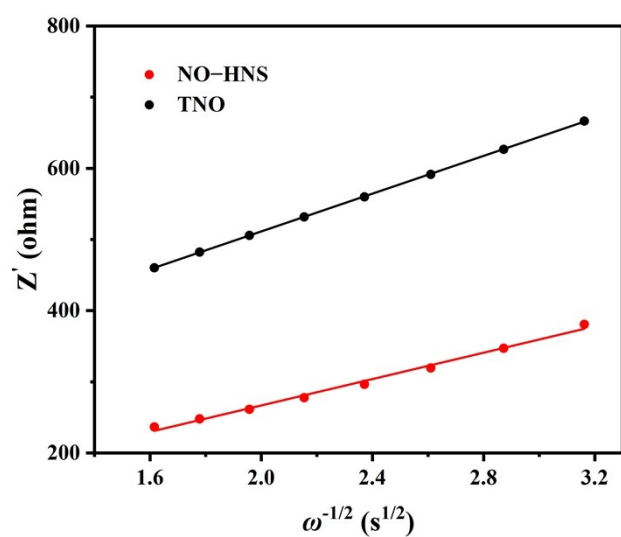


Fig. S7 The fitted lines of the impedance versus $\omega^{-1/2}$ for NO-HNS and TNO.

Supplementary References

1. G. Zhao, L. Zhang, J. Lv, C. Li and K. Sun, *J. Mater. Chem. A*, 2016, **4**, 1399–1407.
2. O. Mizrahi, N. Amir, E. Pollak, O. Chusid, V. Marks, H. Gottlieb, L. Larush, E. Zinigrad and D. Aurbach, *J. Electrochem. Soc.*, 2008, **155**, A103–A109.
3. Y. Yao, L. Zhang, X. Bie, H. Chen, C. Wang, F. Du and G. Chen, *Chem. - A Eur. J.*, 2017, **23**, 17935–17939.
4. X. Miao, Z. Chen, N. Wang, Y. Nuli, J. Wang, J. Yang and S. ichi Hirano, *Nano Energy*, 2017, **34**, 26–35.
5. A. Byeon, M. Q. Zhao, C. E. Ren, J. Halim, S. Kota, P. Urbankowski, B. Anasori, M. W. Barsoum and Y. Gogotsi, *ACS Appl. Mater. Interfaces*, 2017, **9**, 4296–4300.
6. Q. Miao, Y. NuLi, N. Wang, J. Yang, J. Wang and S. I. Hirano, *RSC Adv.*, 2016, **6**, 3231–3234.
7. S. Su, Y. NuLi, Z. Huang, Q. Miao, J. Yang and J. Wang, *ACS Appl. Mater. Interfaces*, 2016, **8**, 7111–7117.
8. S. Su, Z. Huang, Y. Nuli, F. Tuerxun, J. Yang and J. Wang, *Chem. Commun.*, 2015, **51**, 2641–2644.
9. W. Pan, X. Liu, X. Miao, J. Yang, J. Wang, Y. Nuli and S. ichi Hirano, *J. Solid State Electrochem.*, 2015, **19**, 3347–3353.
10. N. Wu, Z. Z. Yang, H. R. Yao, Y. X. Yin, L. Gu and Y. G. Guo, *Angew. Chemie - Int. Ed.*, 2015, **54**, 5757–5761.